This is the author's version of an article that has been published in this conference. Changes were made to this version by the publisher prior to publication. The final version is available at http://dx.doi.org/10.1109/EPEPS.2017.8329706

Design Optimization of a Planar Spiral Inductor Using Space Mapping

Felipe de J. Leal-Romo [1,2], Marisol Cabrera-Gómez[1,2], José E. Rayas-Sánchez[2], and Daniel M. García-Mora[1]

[1]Intel Guadalajara Design Center
Zapopan, Jalisco, 45019 México
[2]Department of Electronics, Systems, and Informatics, ITESO – The Jesuit University of Guadalajara
Tlaquepaque, Jalisco, 45604 México
e-mail: felipe.de.jesus.leal.romo@intel.com

***Abstract* — This paper addresses the implementation of a computationally efficient optimization technique for designing structures simulated in 3D electromagnetic field solvers. A probe of concept is done by the EM-based optimization of a planar spiral inductor for high-power applications. The optimization technique employed is based on space mapping (SM) methods, more specifically on the Broyden-based input space mapping algorithm. Our optimization results confirm the efficiency of the proposed approach.**

***Index Terms* — aggressive space mapping, APLAC, coarse model, driver, fine model, full wave simulator, inductor, lumped elements, optimization, PowerSI 3D EM.**

I. Introduction

During the last three decades, full-wave electromagnetic (EM) field solvers have become increasingly popular in high-speed electronics design. Some of the most common computational techniques employed to solve such complex problems are: finite elements method (FEM) [1], method of moments (MoM) [2], finite integration technique (FIT) [3], among others. One of the most recent 3D FEM tools introduced to the market is Cadence® Sigrity™ PowerSI® 3D EM (PSI-3D) [4], intended for power and signal integrity of IC packages and PCBs. Aiming at developing a practical tool for the design optimization of such large circuits, in this paper we propose, as a proof of concept, a computationally efficient automated approach to optimize the geometry of spiral inductors simulated in PSI-3D. We first describe the spiral structure of interest [5]. Then, we implement the selected spiral inductor in PSI-3D, comparing our simulation results with those in [5]. The resultant PSI-3D model, which is highly accurate but computationally expensive, is taken as our fine model in the context of space mapping optimization [6]. Next, we implement the same inductor in a high-frequency circuit simulator, which is exploited as a coarse model (very fast, but insufficiently accurate). We develop adequate Matlab drivers for these fine and coarse models. Finally, we employ the Broyden-based input space mapping algorithm, better known as aggressive space mapping (ASM) [7,8], as the selected optimization technique to fine tune the geometrical dimensions of the spiral inductor in an automated and efficient manner.

II. Description of the Spiral Inductor Structure

As mentioned before, the selected spiral inductor is intended for relatively high-power applications [5]. Its main geometrical dimensions are shown in Fig. 1. This inductor has 1.5 turns, it is built with copper and utilizes 99.5% pure Alumina (Al_2O_3) as substrate material. Its complete dimensions and material properties are shown in Table I.

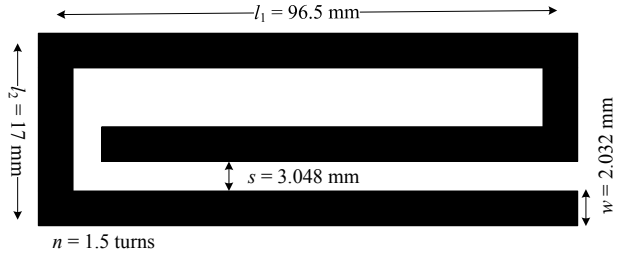

Fig. 1. Spiral Inductor's dimensions for power applications [5].

TABLE I
SPIRAL INDUCTOR PHYSICAL PARAMETERS

Parameter's Name	Initial Value	Final Value
l_1 (mm)	96.5	83.11
l_2 (mm)	17	16.22
s (mm)	3.048	4.48
w (mm)	2.032	16.59
H (mm)	2.54	2.54
t (mm)	0.3048	0.3048
n (turns)	1.5	1.5
ε_r (Al_2O_3)	9.8	9.8
ρ (CuAu)	0.7066	0.7066
σ (S/m)	5.8×10^7	5.8×10^7
$\tan\delta$	0.0001	0.0001

III. Fine Model Implementation in PSI-3D

In this section, we describe the implementation of the planar spiral inductor structure in PSI-3D[1], which is used as our fine model to optimize the geometrical dimensions of this inductor.

The inductor is contained inside a boundary box at least three times taller than the total substrate height plus the inductor and the reference plane, and two times wider and larger than the spiral inductor structure, such that the electromagnetic fields in the structure do not interact with the enclosing box. Two 50-Ω lumped ports perpendicular to the

[1] PowerSI 3D-EM v17.0.0.12061.80497, Cadence Design Systems, Inc., San José, CA, 2016.

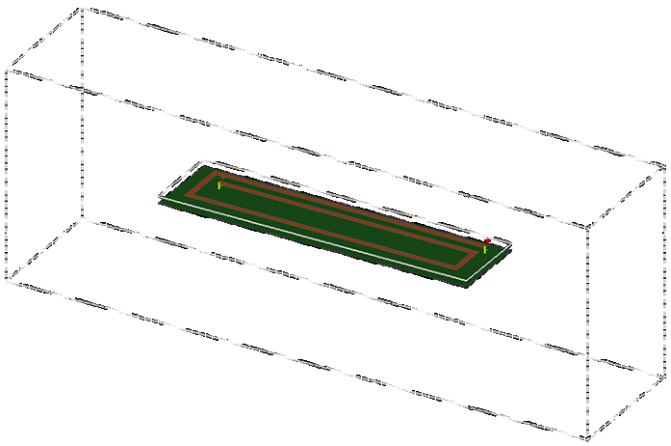

Fig. 2. Implementation of the 1.5 turns spiral inductor in PSI-3D (fine model).

TABLE II
SONNET *VS* PSI-3D RESULTS

Simulator	L (nH) @ 13.5 MHz	f_r (MHz)
Sonnet [5]	132.78	92.5
PSI-3D	130.5	89.12

input and output of the inductor are employed. Finally, for the structure discretization we selected a zero order basis function to generate the mesh.

The inductance value of interest is measured at 13.5 MHz, while the resonance frequency f_r is expected to happen at around 90 MHz.

One simulation (one frequency sweep from 100 Hz to 1 GHz with 141 frequency points, including the construction of the initial mesh, one adaptive mesh iteration, with two as the minimum number of converged iterations per simulation) of this inductor in PSI-3D consumes 5:47 minutes using a Xeon® computer server with 1.5 TB of RAM.

Table II summarizes the parameters obtained in our PSI-3D simulation against the parameters reported from the simulation in [5]. As it is observed in Table II, both numerical results are quite similar. In our case, the inductance measured at 13.5 MHz is off by approximately 2 nH (1.7% difference) and there is a small difference of almost 3 MHz in the resonance frequency (3.6%), with respect to Sonnet's simulation results reported in [5]. These slight discrepancies in the results can be attributed to the nature of the simulators employed, including the different types of excitation ports. In our case, we used a 3D FEM solver, while [5] employs Sonnet, a 2.5D tool that uses the MoM.

IV. Coarse Model Implementation in APLAC

Here we describe the development of the coarse model to be used in our ASM algorithm, which is created in APLAC[2], a high-frequency circuit simulator, with the implementation shown in Fig. 3. We assume the same material properties as well as the same initial geometrical dimensions as those used for the fine model.

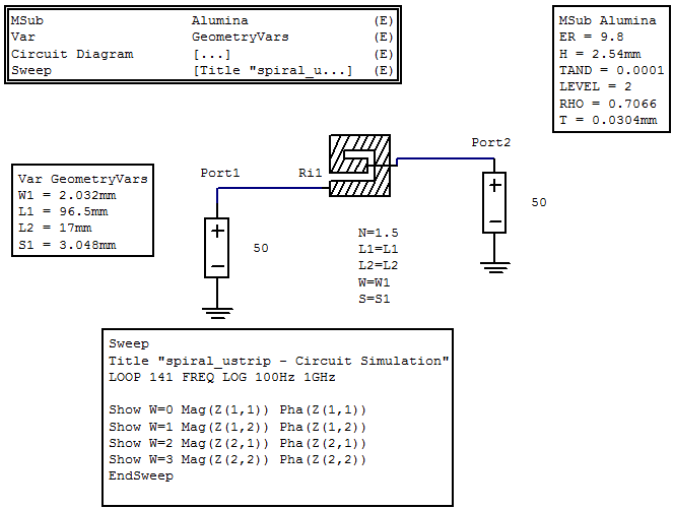

Fig. 3. Implementation of the 1.5 turns spiral inductor in APLAC (coarse model).

Since APLAC utilizes parameter RHO (ρ) to define the normalized resistivity of the metal (copper) with respect to the resistivity of gold, we included this parameter in our simulation settings, as illustrated on Fig. 3 and in Table I. One single frequency sweep of this coarse model takes less than a second using the same server computer used for the fine model.

V. Optimizing the Spiral Inductor with Space Mapping

To test our optimization algorithm, the spiral inductor is optimized by implementing the ASM algorithm [7] in Matlab[3], as depicted in Fig. 4. This algorithm starts by optimizing the coarse model (APLAC circuit) of the original structure, $\boldsymbol{R}_c(\boldsymbol{x}_c)$, to optimally satisfy some given specifications. The coarse model responses are in $\boldsymbol{R}_c$, while the coarse model design parameters are in $\boldsymbol{x}_c$. Then, the optimal design of the coarse model, $\boldsymbol{x}_c^*$, is introduced as the new geometrical parameters into PSI-3D, to run a simulation of the fine model $\boldsymbol{R}_f(\boldsymbol{x}_f)$. With this information, the algorithm reads the S-parameters from the fine model and converts them into Z-parameters to obtain the equivalent AC resistance (R_{AC}) and AC inductance (L_{AC}) parameters, which are the responses of interest contained in vector $\boldsymbol{R}_f$. Next, the coarse model design parameters are extracted such that the corresponding coarse model responses match the current fine model responses. If the extracted parameters are sufficiently close to the optimal coarse model design, the algorithm ends, otherwise, it continues by predicting the new fine model design parameters from Broyden's formula [9] to update the local mapping's Jacobian [8], simulating again the PSI-3D structure with the new

[2] APLAC, ver. 8.1 (formerly APLAC Solutions Corp.), NI AWR Design Environment, El Segundo, CA 90245, USA.

[3] MATLAB, Version 8.5.0.197613, The MathWorks, Inc., 3 Apple Hill Drive, Natick MA 01760-2098, 2015.

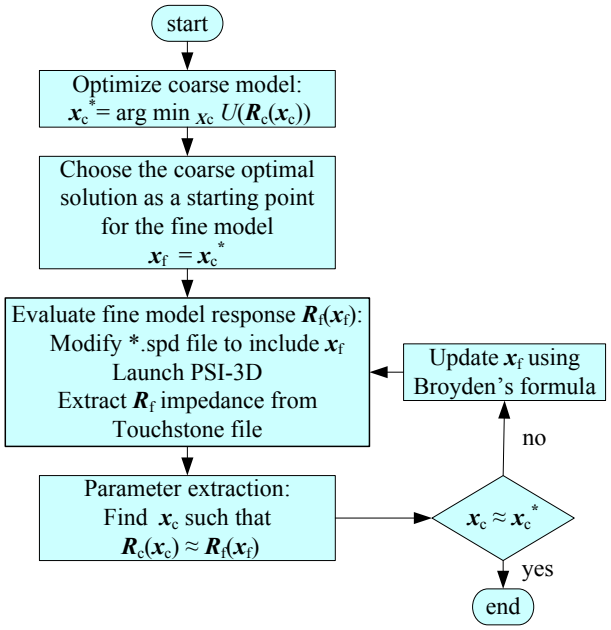

Fig. 4. Aggressive Space Mapping (ASM) algorithm as implemented in Matlab.

geometrical parameters.

A. Matlab Drivers for APLAC and PSI-3D

It is clear that this optimization algorithm requires efficient drivers for both the coarse and fine models. In our case, the coarse model (APLAC) is directly driven from Matlab, while the fine model (PSI-3D) is driven from Matlab as well, but through a driver without graphical user interface (GUI) usage. This feature accelerates the process by not having to load the project for graphical display, since this operation takes long enough to impact the overall execution time.

B. Design Specifications and Optimization Results

To comply with our own high-power design, the problem was formulated to meet the following specifications:

$$L_{AC} \le 115 \text{ nH for } 10 \text{ MHz} \le f \le 16 \text{ MHz} \quad (1)$$

$$R_{AC} \ge 90 \text{ m}\Omega \text{ for } 100 \text{ HZ} \le f \le 1 \text{ kHz} \quad (2)$$

The optimization variables are $\boldsymbol{x} = [w \;\; l_1 \;\; l_2 \;\; s]^T$, keeping fixed the preassigned parameters $\boldsymbol{y} = [H \;\; t \;\; n \;\; \varepsilon_r \;\; \rho \;\; \sigma \;\; \tan\delta]^T$.

As a result of applying ASM, the structure was optimized with 181 APLAC runs and only 8 PSI-3D runs. Final dimensions of this structure are shown in Table I. During the execution of this optimization method, no GUI interface was required (except for the initial creation of the spiral inductor structure). In Fig. 5, we display the relative error of $\boldsymbol{R}_f(\boldsymbol{x}_f) = [L_{AC} \;\; R_{AC}]^T$ along the 8 PSI-3D runs; we meet the desired target response described by (1) and (2) with an error tolerance smaller than 5×10^{-3} in 8 fine model simulations.

VI. Conclusion

Our proposed optimization methodology was tested with the successful implementation of the aggressive space mapping method to fine tune the geometry of the spiral inductor structure using APLAC's equivalent circuit as the coarse model and PowerSI® 3D EM as the fine model. The optimization process achieved desired results for L_{AC} and R_{AC} in specific frequency ranges, with a few iterations of the fine model, while the coarse model required more than a hundred of simulations to achieve the desired goal, which are excecuted in a negligible time.

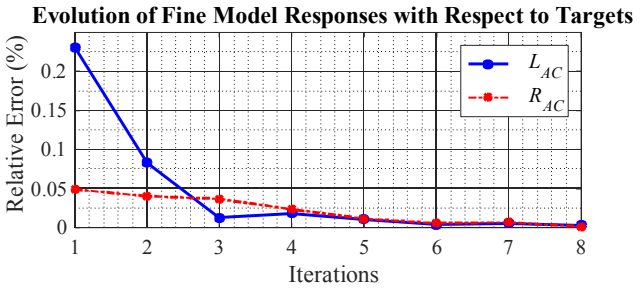

Fig. 5. Relative error of the fine model's L_{AC} and R_{AC} with respect to target values.

Acknowledgement

This work was supported in part by CONACYT (*Consejo Nacional de Ciencia y Tecnología*, Mexican Government) through a scholarship granted to F. J. Leal-Romo.

References

[1] P. Silvester, "A general high-order finite-element waveguide analysis program," *IEEE Trans. Microwave Theory Techn.*, vol. 17, pp. 204-210, 1969.

[2] R. F. Harrington, "Matrix methods for field problems," *Proc. IEEE*, vol. 55, pp. 136-149, 1967.

[3] J. E. Lebaric and D. Kajfez, "Analysis of dielectric resonator cavities using the finite integration technique," *IEEE Trans. Microwave Theory Techn.*, vol. 37, no. 11, pp. 1740-1748, Nov 1989.

[4] Cadence Design Systems, Inc. (2016). *Sigrity PowerSI 3D EM Extraction option* [Online]. Available: https://www.cadence.com/content/cadence-www/global/en_US/home/tools/ic-package-design-and-analysis/si-pi-analysis-point-tools/sigrity-powersi-3d-em-extraction-option.html.

[5] A. Eroglu, "Planar inductor design for high power applications", *Progress in Electromagnetics Research B*, vol. 35, pp. 53-67, Oct. 2011.

[6] J. W. Bandler, Q. Cheng, S. A. Dakroury, A. S. Mohamed, M. H. Bakr, K. Madsen and J. Søndergaard, "Space mapping: the state of the art," *IEEE Trans. Microwave Theory Tech.*, vol. 52, no. 1, pp. 337-361, Jan. 2004.

[7] J. W. Bandler, R. M. Biernacki, S. H. Chen, R. H. Hemmers, and K. Madsen, "Electromagnetic optimization exploiting aggressive space mapping," *IEEE Trans. Microw. Theory Techn.*, vol. 41, no. 12, pp. 2874-2882, Dec. 1995.

[8] J. E. Rayas-Sanchez, "Power in simplicity with ASM, tracing the aggressive space mapping algorithm over two decades of development and engineering applications," *IEEE Microw. Mag.*, vol. 17, no. 4, pp. 64-76, Apr. 2016.

[9] C. G. Broyden, "A class of methods for solving non-linear simultaneous equations", *Math. Comp.*, vol. 19, pp. 577-593, 1965.